THE PRESSURE DEPENDENCE OF THE DIELECTRIC CONSTANT AND ELECTRICAL CONDUCTIVITY OF SINGLE CRYSTAL URANIUM DIOXIDE

R.N. HAMPTON [1], G.A. SAUNDERS [1], J.H. HARDING [2] and A.M. STONEHAM [2]

[1] *School of Physics, University of Bath, Claverton Down, Bath BA2 7AY, United Kingdom*
[2] *Theoretical Physics Division, Harwell Laboratory, AERE Harwell, Oxfordshire OX11 0RA, United Kingdom*

Complex impedance techniques, within the frequency range 10 Hz to 1 MHz, have been used to make high pressure studies of monocrystalline uranium dioxide at ambient temperature. These techniques have shown that for frequencies below 40 MHz the electrical properties of high pressure samples are dominated by a boundary layer. The impedance methods have enabled us to make the first determination of the pressure dependence of the static dielectric constant of uranium dioxide within the boundary layer. The experimental pressure dependence (-0.03 kbar^{-1}) is in reasonable agreement with that calculated (-0.02 kbar^{-1}) using standard interatomic potentials. We have also measured the conductivity in the boundary layer as a function of pressure (2.5 μS kbar^{-1}). The pressure dependences of the conductivity and the dielectric constant have been used to obtain an estimate of the carrier binding and hopping energies, which have then been compared with values predicted using the shell model.

1. Introduction

Primarily because of its use as a fuel for nuclear reactors, uranium dioxide has attracted considerable experimental and theoretical attention. Uranium dioxide is a high melting-point (3120 K) fluorite-structured oxide, which can be described electrically as a Mott insulator, a poor semiconductor, or a fast ion conductor depending upon the temperature range of interest! To try to overcome the difficulties of experiment alone, experimental and theoretical work has proceeded hand-in-hand, with theoretical models needing experimental input [1,2], and experimental work often directed by theoretical predictions. Much of the theoretical work involves the use of interatomic potentials [3–5], which are determined from fitting to experimental data. The accuracy of a potential can also be tested by considering its ability to reproduce elastic stiffness, dielectric constant and other data. Thus an experimental determination of the pressure dependence of the dielectric constant provides a useful test of the ability of a chosen potential to predict the effect of pressure on other properties of uranium dioxide. Further, the pressure dependence of the electrical conductivity can be measured simultaneously with the dielectric constant. Knowledge of the conductivity is of particular relevance to understanding the specific heat and the thermal

conductivity [1,2] at high temperatures. We know of no other electrical conductivity data at high pressures.

Previous dielectric constant determinations showed certain inconsistencies [6–13]. The initial work [11] indicated that these inconsistencies extended to electrical conductivity measurements in the form of an anomalous frequency dependence, which had not been reported previously [14,15]. These problems have now been resolved [19] by the use of complex impedance plane analysis [16–18] to deal with the data produced using ac measurement techniques. The previous inconsistencies derived from an incorrect description of the equivalent electrical circuit used originally to analyse the data [19]. In fact the correct circuit comprises two parallel combinations of conductances and capacitances connected in series. Plausibly, one combination represents the bulk crystal and the other a surface boundary layer. The thickness of the boundary layer has been estimated from capacitance versus voltage measurements, assuming it can be described as a Schottky barrier. This approach proved successful, the calculated boundary layer thickness of 600 Å giving a dielectric constant of 33. The experimental results lend support to the assertion that the boundary layer arises from band bending associated with deposition of a metal contact onto a Mott insulator.

2. Experimental details

Electrical admittance measurements were made on small single crystals of UO_2 using a Hewlett Packard B4905 Impedance Analyser and the ac techniques described elsewhere [16–19]. The high pressures used in this work were produced in the tetrahedral anvil apparatus of STL Harlow. The samples were encapsulated in epoxy resin and housed in a pyrophyllite tetrahedron. The tetrahedron was then loaded equally on each face, causing the system to exert a hydrostatic pressure on the sample. The pressures that could be attained using this technique were in the range 25 kbar to 70 kbar.

3. Establishment of the equivalent circuit

Previous electrical measurements on plate geometry samples of UO_2 [19] had established the presence of a boundary layer which manifested itself in the equivalent electrical circuit (fig. 1). Of necessity the samples used in the present work were small due to the constraints of the pressure cell (1 mm × 1 mm × 0.5 mm). Our earlier work suggests that for samples of this size and geometry the volume effects would not become wholly dominant until the measurement frequency exceeded 40 MHz (well above that available). The boundary properties dominated the admittance data for frequencies up to 2kHz. In that range the equivalent circuit is a single parallel combination of capacitance and conductance due to the boundary layer alone. The boundary layer effects contribute extensively to the electrical properties for frequencies up to 2 MHz.

Data for a circuit of this form are most conveniently interpreted through the use of its complex admittance, with a plot of Y' against Y'' resulting in a straight line. This is shown schematically in fig. 1. The linear form of our present data (fig. 2) is consistent with the equivalent circuit assumed for the low frequencies we have used; contributions from the volume circuit result in a deviation of the data from a straight line for frequencies in excess of 2 kHz. The results show a marked dependence upon the applied test voltage, this being most pronounced at low frequencies. This voltage dependence has been associated with boundary phenomena [16,19]. The inclination of the linear portion of the profile can be accounted for by replacing the ideal capacitor in the equivalent circuit with one with a so-called "universal response" [16,17] where the frequency dependences of the circuit are lumped together in a frequency dependent capacitance $C(\omega)$. The admittance of the circuit
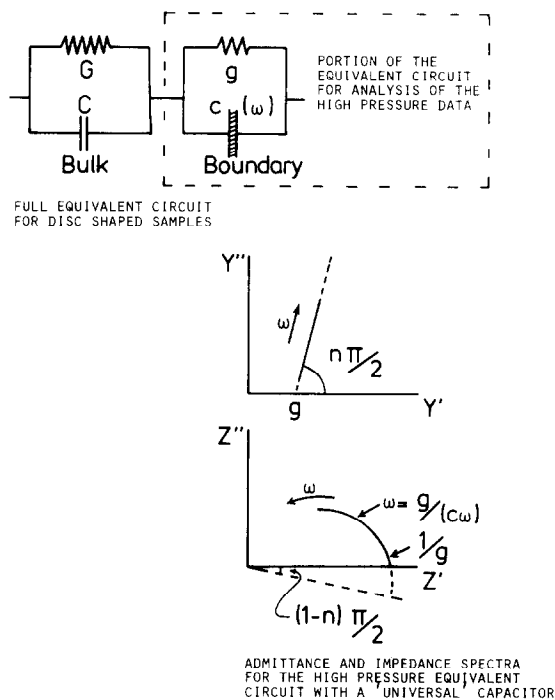

Fig. 1. Complex electrical profiles for an analysis of the admittance data.

can then be described by an expression of the form:

$$Y(\omega) = G + j\omega C(\omega), \tag{1}$$

$$Y(\omega) = G + B(\cos(n\pi/2) + j \sin(n\pi/2))\omega^n. \tag{2}$$

4. Pressure dependence of the electrical conductance

The conductance obtained at an ambient temperature of 300 K from these analyses (fig. 3) shows a sharp increase following the initial application of pressure. This initial change can be attributed to the settling of the contacts on the sample, rather than to any intrinsic behaviour of the material. This interpretation is supported further by the ultrasonic studies [20] in which no pressure-induced phase transitions were found in UO_2 for pressures up to 20 kbar.

The conductance achieves a stable value at a pressure of 30 kbar, beyond which it shows a steady increase with pressure. Previously a dc measurement of the resistance as a function of pressure has been reported [21]. Although both sets of results show that the conductivity increases with pressure, they are at variance in the size of the effect; the present measurements give a value of 2.5 μS kbar^{-1} for dG/dP, whereas the
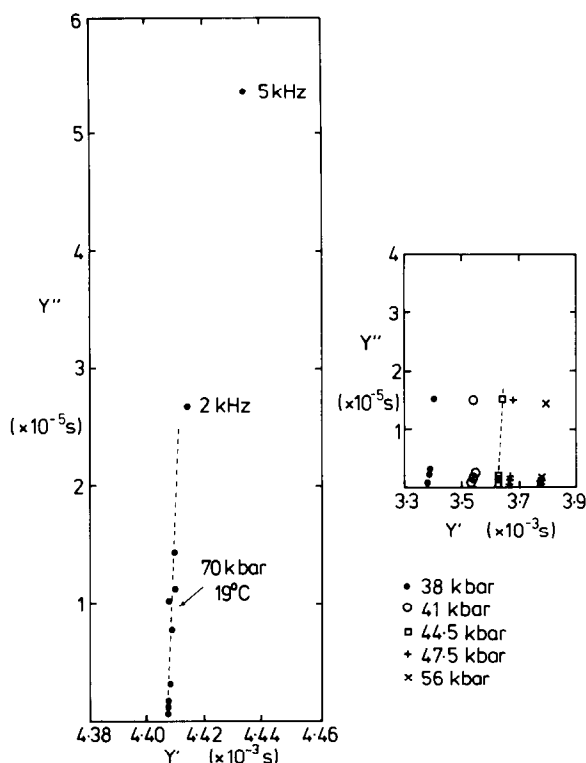
Fig. 2. Admittance profiles of single crystal (Norton) material at selected pressures. The figures indicate the frequency (kHz) of specific admittance points. The solid lines serves as a guide to the eye.

previous data yielded a value of 0.68 μS kbar^{-1}. It is not possible to account for this because full experimental details of the previous work were not available to us.
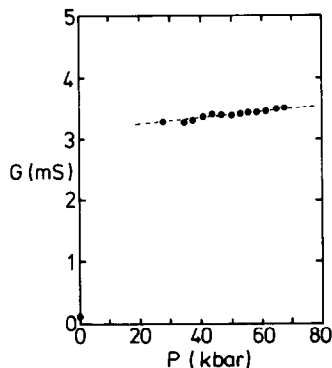

Fig. 3. The dc conductance, obtained from the real admittance intercept, as a function of hydrostatic pressure at an ambient temperature of 300 K.

5. Pressure dependence of the dielectric constant

The sample capacitance was obtained from single-frequency measurements made using a Wayne Kerr B905 Bridge. Conductance data could not be obtained from these measurements as the frequencies used (100 Hz, 1 kHz, 2 kHz and 10 kHz) straddled the boundary-dominant and the mixed boundary-bulk regions, and the two regions were not separable. The dielectric constant was calculated as a function of frequency at selected pressures (fig. 4) from the measurements of the sample capacitance, using the known sample dimensions. The frequency dependence of the dielectric constants calculated directly from the universal capacitor model (eq. (2)), using the value of n calculated from the gradient of the admittance profiles, correlates well with the experimental data. It is interesting to note that the capacitance does not display any of the artefacts exhibited by the conductances measured in the same way.

The dielectric constant is large and very dependent upon frequency. This is consistent with the other low frequency/high temperature measurements made on UO_2 [9–11], and is caused by the dominance of the boundary layer capacitance in this frequency region. Previous work on the boundary layer [19] established its
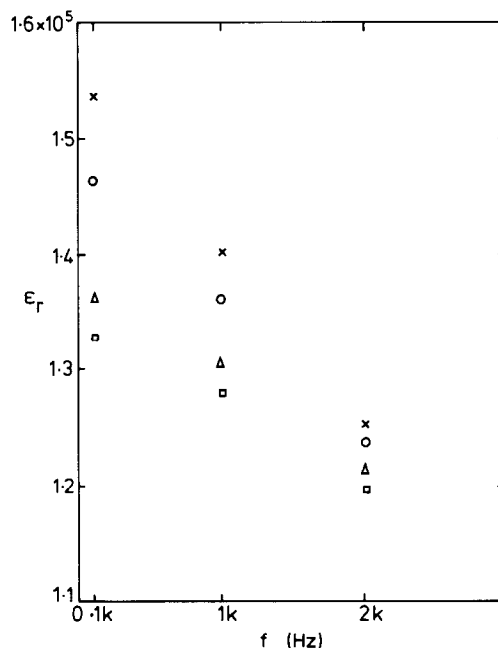

Fig. 4. The dielectric constant, calculated from the measured capacitance on the basis of the sample dimensions, as a function of frequency at selected pressures: ($\times$) 25 kbar, (O) 37.5 kbar, (r$\triangle$) 57.5 kbar and ($\square$) 70 kbar).
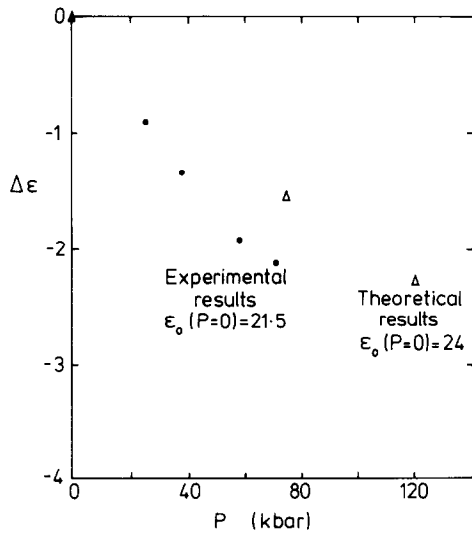
Fig. 5. The dielectric constant deviation ($\Delta\epsilon = \epsilon(P = 0) - \epsilon(P)$) as a function of the applied hydrostatic pressure: (●) experimental results and (△) theoretical results). The dielectric constants were obtained from the data (fig. 4) using 600 Å as the thickness of the boundary layer.

thickness as about 600 Å, this being the correct thickness to use when evaluating the static dielectric constant for these samples at atmospheric pressures. The variation of ϵ_0 with pressure (fig. 5) is calculated from the zero frequency capacitance, obtained by the extrapolation of the data given in fig. 4 and using the thickness of the boundary layer. Our analysis assumes that the thickness of the boundary layer is independent of pressure. The zero pressure dielectric constant calculated in this manner is 21.5. This value for the dielectric constant is lower than that found previously [19] for the boundary layer which was 33. The samples used for the high pressure work had been recently reduced, and the experiments were conducted within two weeks of the reduction, so the difference probably results from stoichiometry differences in the outer boundary region.

6. Comparison with theory

A theoretical calculation, based on a shell model [22] and using the Harwell PLUTO program [3], also shows a decreasing dielectric constant with pressure (fig. 5). The zero pressure values of the experimental and theoretical data differ somewhat; this can be attributed in part to the fact that the previously accepted value of 24 for ϵ_0 had been used to parameterise the interatomic potential [5] and in part to the errors which are inherent

in making capacitance measurements on samples which have a small area to thickness ratio. Thus it is more instructive to note the reasonable agreement between the gradients: -0.03 kbar^{-1} (experimental) and -0.02 kbar^{-1} (theoretical). It needs to be stressed here that the experimental measurements correspond to the effect of hydrostatic pressure on the boundary layer capacitance of nominally stoichiometric (recently reduced) material. The similarity of the dielectric constants measured in the boundary and bulk regions is consistent with the Mott–Schottky description assumed for the boundary layer.

7. Carrier binding energies

The conductance will depend upon the conductivity and various geometrical factors. Its pressure dependence will come from the effects of pressure on the carrier concentration and carrier mobility. If we suppose that the carriers are electronic holes (U^{5+}) [1,2] which may either be free or bound to an oxygen interstitial, it can be expected that the carrier concentration (n) will be proportional to $\exp(-B/kT)$, with B a binding energy which we shall discuss. Further the holes may form electronic small polarons, and their mobility will then have the form [24],

$$\mu = J^2 \exp(-D/kT),\qquad(3)$$

where D is a hopping energy and J an electron transfer matrix element. The pressure dependence now has two main terms. First, there is the effect of changes in ϵ_0 and ϵ_∞ on B and D. Second, there is the effect of the interionic spacing on J. We start by analysing B and D for their dependence on ϵ_0 and ϵ_∞.

In the simplest models, B corresponds to binding by a Coulombic potential screened by the static dielectric constant ϵ_0, so we have $B = b/\epsilon_0$ (where $b = e^2/r$ with r the U^{5+} to oxygen interstitial spacing). Similarly the polaron hopping energy depends upon the ionic polarization (rather than the total polarization) so one expects $D = d(1/\epsilon_\infty - 1/\epsilon_0)$. The dependence of the high frequency dielectric constant on pressure will be neglected, since calculations suggest that it is small. Thus the temperature-dependent factors in the conductance can be written as:

$$\psi = \exp(-d/\epsilon_\infty kT)\exp((d-b)/\epsilon_0 kT).\qquad(4)$$

The pressure dependence at constant temperature gives

$$(1/\psi)(\mathrm{d}\psi/\mathrm{d}P) = (1/\epsilon_0^2 kT)(d-b)(-\mathrm{d}\epsilon_0/\mathrm{d}P).$$
$$(5)$$

Similarly, we can write J with its standard exponential dependence on interionic distance R as a factor

$$\phi = J_0^2 \exp(-2R/q), \tag{6}$$

$$(1/\phi)(d\phi/dP) = 2R/q(-1/R)(dR/dP). \tag{7}$$

Here q is some sort of orbital radius, and its precise interpretation depends on whether one assumes direct U–U interactions or indirect interactions via a common oxygen. One anticipates R is the oxygen–oxygen distance and q is of the order of the size of the 5f orbital, which is normally of the order of a few tenths of an ångström. Since the conductance G is proportional to $\phi\psi$ we have

$$(1/G)(dG/dP)$$
$$= (d-b)/(\epsilon_0 kT)(-1/\epsilon_0)(d\epsilon_o/dP)$$
$$+ 2R/q(-1/R)(dR/dP). \tag{8}$$

Since neither $(d-b)$ nor q, are known a unique solution cannot be found. Nevertheless, we can derive some useful limits.

The analysis can now proceed in three directions. The first option is to neglect the last term in eq. (8), assuming J is insensitive to R. This corresponds to what is often known as the Condon approximation. The analysis gives B and D as a combination and not as separate values. However the Arrhenius energy at low temperatures ($E = B + D = 0.17$ eV) is known with some certainty from the previous conductivity work [14,24,25]. This extra information was used to obtain the separate energies, and leads to the values of 0.026 eV and 0.141 eV for B and D respectively, i.e. the hopping energy is

Table 1
Binding and hopping energies calculated from eq. (8) for selected values of $2R/q$

$2R/q$	Hopping energy (eV)	Binding energy (eV)
0	0.141	0.026
10	0.128	0.042
20	0.114	0.056
30	0.100	0.069
40	0.087	0.083
50	0.074	0.096
60	0.060	0.116
70	0.047	0.123
80	0.033	0.136
90	0.020	0.150

much larger than the binding term. The problem with this first approach (see section 8) is that the binding energy is unacceptably smaller than that predicted and that the standard temperature dependence of D from small polaron theory would indicate too large a high-temperature activation energy. The second approach considers only the last term, and assumes that the variation of J with spacing dominates. This allows a value for $2R/q$ to be calculated. This value of -6.5 for $2R/q$ (so, with $R = 5.45$ Å, q is 1.67 Å) gives the function dimensions for which $d = b$.

Whilst this is somewhat artificial, it is consistent with our conclusion in section 8 that the variation of J is important.

A third approach, which allows both possibilities, is to postulate possible values for $2R/q$ and then to calculate values of B and D (table 1 and fig. 6). The analysis indicates that B and D are adequately fitted by the equations (energies in eV):

$$B = 0.026 + 1.23 \times 10^{-3}(2R/q), \tag{9}$$

$$D = 0.141 - 1.36 \times 10^{-3}(2R/q). \tag{10}$$

Thus the analysis is able to give the range of $2R/q$ for which B, D and $2R/q$ were positive; the range of the binding and hopping energies that are encompassed within the allowed values of $2R/q$ have also been calculated:

0.025 eV < B < 0.17 eV,
0.141 eV > D > 0 eV,
where $B + D = 0.17$ eV,
within the range $0 < 2R/q < 104$.

We shall now consider values of binding and mobility energies.
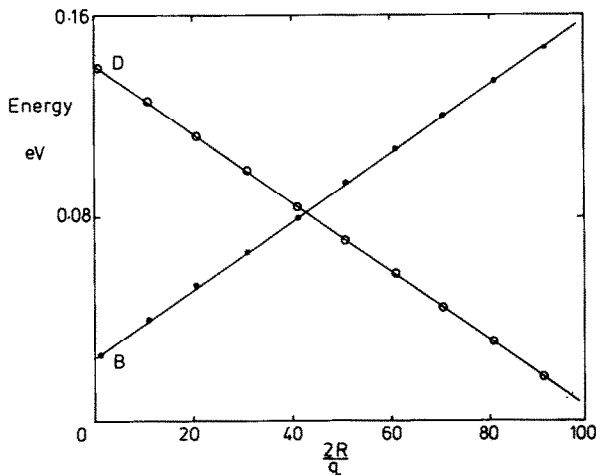

Fig. 6. The binding (●) and hopping (○) energies, calculated from eq. (8), at selected values of $2R/q$.

8. Motion and binding energies

The Harwell HADES codes has been used to estimate the energy needed to ionise an oxygen interstitial cluster, i.e. for the reaction $(O_i^{2-})^x \rightarrow (O_i^{2-})'' + 2h°$, where $(O_i^{2-})^x$ is the oxygen interstitial neutralised by the presence of two bound holes. This energy has been calculated as being about 0.86 eV. If it is assumed that the second hole will be twice as strongly bound as the first (the precise ratio does not prove too important here), the cost of successively ionising each hole is 0.29 eV and 0.57 eV respectively.

We now look at estimates of B and D. We can write down mass action expressions for holes trapped by oxygen interstitials. Thus, if $[O_i^{2-}]^x$ is the concentration of neutral centres with two trapped holes, and $[O_i^h]''$ the concentrations of other charge states, the hole concentration [h] is obtained from

$$\alpha \left[O_i^{2-} \right]^x = [O_i]'[h],$$
$$\beta [O_i]' = [O_i]''[h],$$

where α is proportional to $\exp(-B_1/kT)$ and β to $\exp(-B_2/kT)$, with B_1 (~ 0.29 eV) and B_2 (~ 0.57 eV) the binding energies calculated. However, these should not be compared directly with our previous values of B. Suppose we may ignore the second ionisation, i.e. β negligible. If the only holes present are from ionisation of oxygen interstitials, charge neutrality requires $[O_i^{2-}]' = [h]$ so that overall the hole concentration varies as $\exp[-(B_1/2)/kT]$, i.e. an apparent B of 0.145 eV. If β is small but finite, a term proportional to $\exp(-B_2/kT)$ also appears.

We may also estimate D from the analysis of Hyland and Ralph [2] and the data of Killeen [24]. At high temperatures, the activation energy for the mobility is 0.14 eV. There are some uncertainties about the best value to take, since this figure (which should suffice here) is based on an Arrhenius fit to the conductivity and took the thermopower to be unactivated. However, it is a standard result of small polaron theory that the apparent motion energy falls with temperature. Suitable expressions are given and evaluated by Norgett and Stoneham [26]. For any reasonable parameters one finds effective values of D less than 0.02–0.03 eV. Thus we conclude an apparent activation energy of 0.17 eV (observed) is entirely consistent with the sum of $B_1/2$ (~ 0.145 eV) and D reduced from its high temperature value using small-polaron theory. We also conclude $B \gg D$, i.e. that the binding energy exceeds the (low-temperature) mobility energy, contrary to the first option of section 7. The main effect of pressure must come from the dependence of J on spacing. The values of q needed are somewhat smaller than reasonable, typically 0.112–0.127 Å, rather than 0.5–1 Å, but the value is sensitive both to our results and details of our model used in the interpretation.

9. Conclusion

This work has shown that the ability of the impedance plane technique to describe regions with different electrical properties can be successfully extended to high pressure studies of uranium dioxide. The pressure dependences of the conductance and dielectric constant, obtained in this manner for the boundary layer of the material, are linear. The pressure dependence of the dielectric constant is in good agreement with the theoretical calculations even though the experimental data is derived from the boundary layer of the material. There is also acceptable agreement between the theory and experiment with regard to the carrier binding energy. This work, together with the previous work of three of the authors [19], has verified the correct equivalent circuit for electrical measurements on uranium dioxide and shown that the theoretical techniques designed for use on the bulk material are applicable to the boundary layer. This adds further confirmation to the suggestion that the boundary layer can be considered as a slightly modified form of the bulk uranium dioxide behaving as a Mott–Schottky barrier.

Acknowledgement

References

[1] G. Hyland, J. Nucl. Mater. 113 (1983) 125.
[2] G. Hyland and J. Ralph, High Temp–High Press. 15 (1983) 179.
[3] C.R.A. Catlow and M.J. Norgett, AERE Report, R. 2763 (1976).
[4] C.R.A. Catlow, Proc. Roy. Soc. London A364 (1978) 473.
[5] R.A. Jackson, A.D. Murray, J.H. Harding and C.R.A. Catlow, Philos. Mag. A53 (1986) 439.
[6] J.D. Axe and G.C. Pettit, Phys. Rev. 151 (1954) 676.
[7] A. Briggs, Report to International Atomic Energy Agency, Vienna (1964).
[8] K. Gesi and J. Tateno, Jpn J. Appl. Phys. 8 (1969) 1358.
[9] D.J. Huntley, Can. J. Phys. 44 (1966) 2952.

[10] S. Iida, Jpn J. Appl. Phys. 4 (1965), 833.

[11] N. Hampton, E.A. Saunders, G.A. Saunders, D. Vigar and A.M. Stoneham, J. Nucl. Mater. 132 (1985) 156–159.

[12] J. Schoenes, Phys. Rep. 63 (1980) 301.

[13] J. Tateno, J. Chem. Phys. 81 (1984) 6130.

[14] J.L. Bates, C.A. Hinman and T. Kawada, J. Am. Ceram. Soc. 50 (1967) 652.

[15] H.M. Lee, J. Nucl. Mater. 56 (1975) 81.

[16] A.K. Jonscher, J. Mater. Sci. 13 (1978) 553.

[17] A.K. Jonscher, Dielectric Relaxation in Solids (Chelsea Dielectrics Press. London, 1983) p. 62–95.

[18] A.K. Jonscher and J.M. Reau, J. Mater. Sci. 13 (1978) 563.

[19] N. Hampton, G.A. Saunders and A.M. Stoneham, J. Nucl. Mater. 139 (1986) 185–190.

[20] I.J. Fritz, J. Appl. Phys. 47 (1976) 4353.

[21] S.N. Vaidya, C. Karunakeran, M.D. Karkhanavala and R. Krishnan, J. Nucl. Mater. 60 (1976) 339.

[22] C.R.A. Catlow, Proc. Roy. Soc. London A353 (1977) 533.

[23] N.F. Mott and E.A. Davis, Electronic Processes in Non-Crystalline Materials (Oxford University Press, 1971).

[24] J.C. Killeen, J. Nucl. Mater. 88 (1980) 185.

[25] Z.A. Munir, Int. J. Thermophys. 2 (1981) 177.

[26] M.J. Norgett and A.M. Stoneham, J. Phys. C6 (1973) 238.